EMBEDDED ELECTROMAGNETIC ADCS SYSTEM FOR LOW ORBIT CUBESAT

A Thesis

by

Merve Kahyaoğlu

Submitted to the

Graduate School of Sciences and Engineering
In Partial Fulfillment of the Requirements for
the Degree of

Master of Science

in the
Department of Electrical and Electronics Engineering

Özyeğin University
August 2020

EMBEDDED ELECTROMAGNETIC ADCS SYSTEM FOR LOW ORBIT CUBESAT

Approved by:

Asst. Prof. Ahmet Tekin, Advisor,
Department of Electrical and
Electronics Engineering
Özyeğin University

Asst. Prof. Evşen YANMAZ
ADAM,
Department of Electrical and
Electronics Engineering
Özyeğin University

Assoc. Professor Radosveta Ivanova
Sokullu
Department of Electrical and
Electronics Engineering
Ege University

Date Approved: 18 August 2020

To My Parents,

İsmail and Hatice Sayar

for their patience and support in all aspect of my life.

And most of all,

I owe my deepest gratitude to my husband, Mr. Mert Kahyaoğlu,

for his affection, encouragement, understanding and patience.

and

My dear niece Melis Sayar, wishing to inspire her future

ABSTRACT

In this study, an embedded custom CubeSat electromagnetic attitude determination and control system that takes a minimum headroom is described. It is designed to provide a fine control in multiple axes. Experimental measurements were conducted by hanging it in a lab environment to evaluate the proposed ideas in a prototype body. 3U CubeSat with dimensions of 10cm x 10cm x 30cm is designed and 3D prototyped with plastic. The outer structure of the aircraft is sized precisely to comply with the standards and custom rather inner two identical half structures are mounted with 45 degrees offset in the main CubeSat vertical plane. Thanks to this custom core structure, the magnetic coils mounted in the body frame structure can create forces in 24 different directions on 12 different surfaces. In the system, which is split in the middle 15 cm away from the tips, the coils that are embedded in the frame edges create forces in many different directions if ignited. Different amounts of torque and directional forces are obtained by pushing different amounts of electrical current into the coils. A stronger rotational orientation is obtained under the influence of the coil windings wrapped from corner to corner. The operation of the system has been verified experimentally and results from an initial prototype have been discussed. A mildly loaded 3D printed prototype tumbling with 18 rad/sec angular speed could be stabilized in the desired position in just 495 seconds burning average power of 600 mW.

ÖZETÇE

Bu çalışmada bir küp uydu için yönelim belirleme ve yönelim kontrolü için elektromanyetik alan kuvvetlerini kullanarak manyetik tork üretici tasarımı yapılmıştır. Tasarımda manyetik alan oluşturacak bakır tellerin küp uydu gövdesindeki mekanik yapının içerisine gömülü sarılmasıyla elde edilir. Bu sayede bir küp uydu içerisinde yönelim kontrolü oluşturmak için ekstradan bir alan kaplamaz. Önerilen fikir bu tez çalışmasında test düzeneği ile denenmiştir. Deneme sonuçları grafik olarak etkisi gösterilmiştir. Küp uydu standartlarında olan 3U 100x100x300mm boyutlarında 3 boyutlu yazıcı ile üretilen gövde ile ilk deneme yapılmıştır. Küp uydu sisteminde yüksekliğinin yarısında 45 derece fark oluşturularak birleştirilen gövde yapısında 12 farklı yüzeyden 24 farklı yönde kuvvet oluşturabilmektedir. Manyetik alan için sarılan bakır teller ile oluşturulmak istenen kuvvetler için farklı miktarda elektrik akımı iletilerek doğrusal bir oranda tork elde edilir. Sistemin çalışması deneysel olarak doğrulanmıştır ve küp uyduya dışarıdan uygulanan bozucu kuvvetin en yüksek değeri olan 18 rad/sn açısal hızın 495 saniyede ortalamada 600mW harcanan güç ile istenen konumda sabitlenebildiği görülmüştür.

ACKNOWLEDGMENTS

I would like to express my very great appreciation to Mr. Dr. Ahmet Tekin for his valuable and constructive suggestions during the planning and development of this research work. His willingness to give his time so generously has been very much appreciated.

I wish to thank various people for their contribution to this project; Mr. Ahmet Sayar and Mrs. Canan Sayar for their valuable mechanical design support on this project.

TABLE OF CONTENTS

LIST OF TABLES

,

LIST OF FIGURES

CHAPTER I

INTRODUCTION

The design and development of small size Cube Satellite's (CubeSat) have been accelerated significantly with the emerging applications in aerospace engineering and science. Design is becoming increasingly difficult, mainly due to the cost and design constraints imposed by mission objectives [1]. Hence, the Attitude Determination and Control System (ADCS) requirements and architecture are guided by task objectives when dealing with challenges such as limited volume and power availability [2].

The proposed CubeSat dimensions are designed not to exceed the standard 3U size of 10cm x 10cm x 30cm [3]. Small size and a limited area of the satellites are customized to offer solutions that reduce the overall cost. This fact makes it possible to launch extra multiple satellites in a single launch. As a result, low-cost commercial and research mission satellites have become quite popular. The most important challenge for the emerging CubeSat's is the requirement to perform high-efficiency operations within an extremely limited volume. The masses and the volumes of the subsystems used in CubeSat should be as small as possible. Besides, their functionality needs to be satisfied efficiently.

There are various methods used to orient satellites in orbits such as reaction wheels, magnetorquer, or gas outlets. One of the most effective methods is the force against the magnetic field created by the current pushed into the coil with magnetorquer. In addition to being light, magnetic torques are used in small satellites because of their low power consumption and their continuous usage. Also, it does not require any maintenance since it does not create mechanical friction. That is why most Low Earth Orbit (LEO) satellites involve magnetorquer and utilize Earth's magnetic field for ADCS purposes. The particular magnetorquer technique discussed in this work is integrated inside the body frame and does not occupy any extra space.

In order to use this force efficiently in the satellite, it is important to occupy minimum volume and leave more space for the sensors and other electronic circuits in the satellite [4-6].

In Table 1, the standardized dimensions and weight measurements of the cube satellites are given in a table. These standard values provide convenience for all developers in designs. Standardization is very important for the creation of suitable satellite designs, especially for rocket carrier developers.

Table 1: Cube satellite sizes. [2]

Cube Satellite	Dimensions (mm)	Weight Range (kg)
1U	100x100x100	0 - 1.3
2U	100x100x200	0 - 3
3U	100x100x300	0 - 4

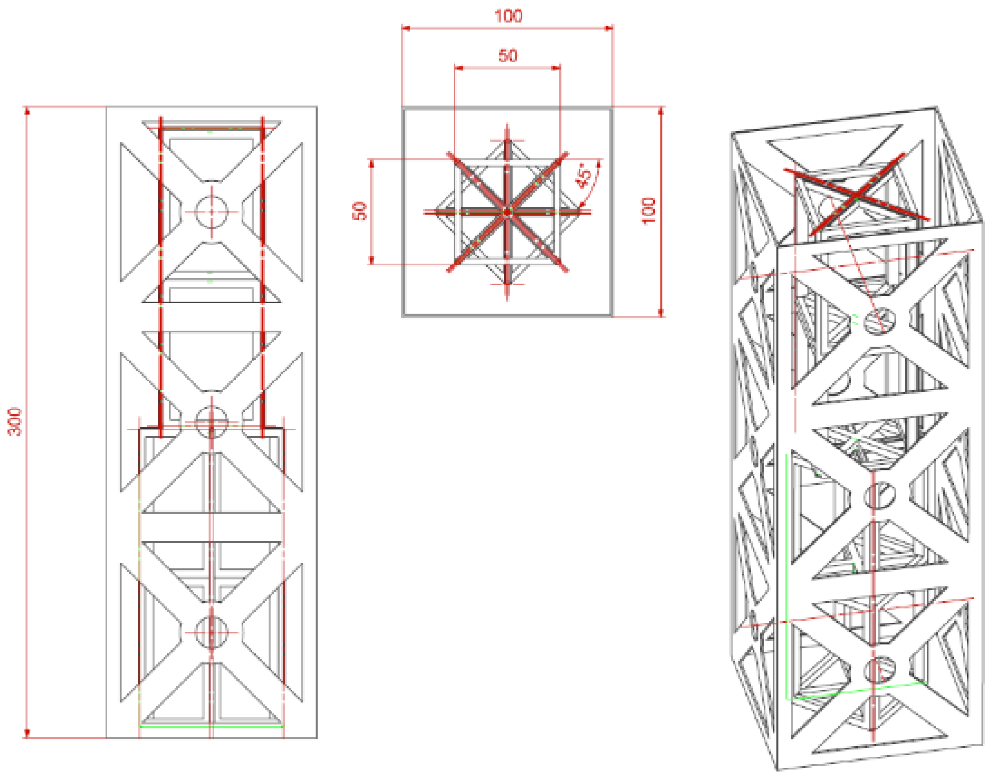

Figure 1: 3U CubeSat body

In this studies, we describe the ADCS hardware and software in development for the CubeSat mission which is 5cm x 5cm x 30 cm length and mounted in the inner structure of the satellite that has been rotated 45 degrees from the main vertical plane starting from 15th centimeter measured from the tips. The 45-deg symmetric rotation around the center of mass is done immediately after deployment from the rocket. An overview from outside of CubeSat 3U is shown in Figure 1. This custom volume allocation does not only increase antenna and solar power area efficiency but also generates more sensitive forces for ADCS systems due to finer resolution control. Novel to our approach is coil windings were mounted in the CubeSat body with cross windings around to the center of mass. A more sensitive structural test was performed with less force by changing the current direction of 12 different windings inside the body. The force is created in 24 directions which produce faster and more efficient direction response provided with the opposing forces ignited in the most appropriate torque generating coils only. Creating moments from multiple directions symmetrically around the center of mass provides more precise orientation accuracy. This distributed fine control is not the case for standard off-the-shelf ADCS systems which need to be mounted at a fixed location. On one hand if it was close to the center of mass, it needs extra power to actuate, and if far away towards the tips, then it creates rather an imbalance in another dimension.

Cross wraps in the proposed structure can also be used as a fluxgate magnetometer so that, it may not be needed to use an additional magnetometer sensor on CubeSat.

1.1 Overview of the CubeSat

One of the most important developments in electronics, communication, and space technology is the satellites operated by placing them in orbits around the world. This is because these satellites used in technology have advantages such as having quite a large coverage area, broadcast capacity, flexibility in bandwidth, and portability. In the last century, there has been a lot of interest in space technologies due to communication and scientific studies. Not only space in exchange for improvements made large investments for the development of space technology has also been advances in other fields of engineering. For instance, there have been significant advances in communication, scientific experiments, imaging technologies, orientation systems, and discovery systems. Due to the large size and cost of the first satellite structures, it is desired to use more special structures for special purposes. Instead of having more than one payload in large systems, there are advantages to only sending specialized payloads separately. These special structures were more compact than previous satellites and, although varying according to the purpose, they were smaller in size. Another factor in the change of dimensions and weight is the reduction of launch cost. Due to the high launch cost of large-sized satellites, a very high-cost investment is required for a single mission, and a single organization must bear this cost, whereas, in cube satellite development, the cost is divided according to the number of studies.

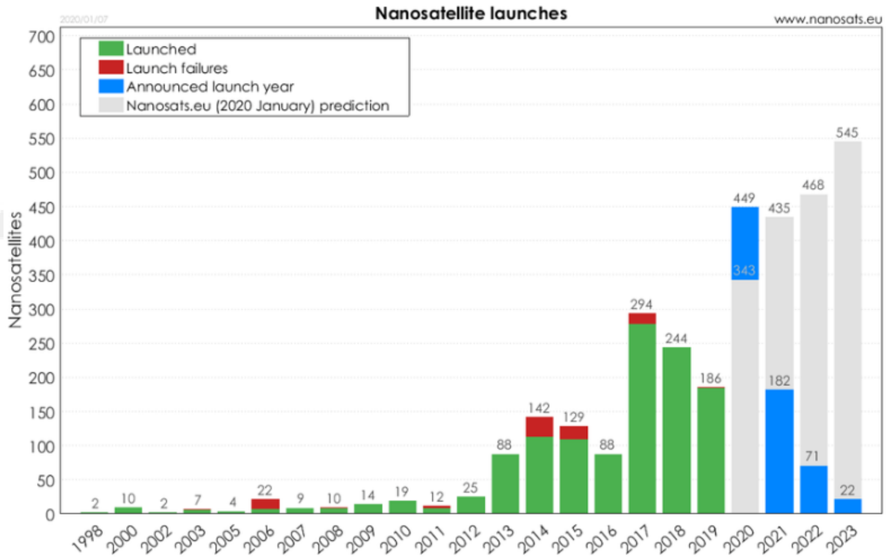

Figure 2: Yearly launched and planned CubeSat’s [7]

According to the data of Nanosats, the number of studies in this field will increase exponentially in the future. The graph shown in Figure 2 shows the number of Nano satellites planned to be sent from the past to the present and until 2023. Approximately 2500 more CubeSat’s are planned to be sent in the next 6 years.

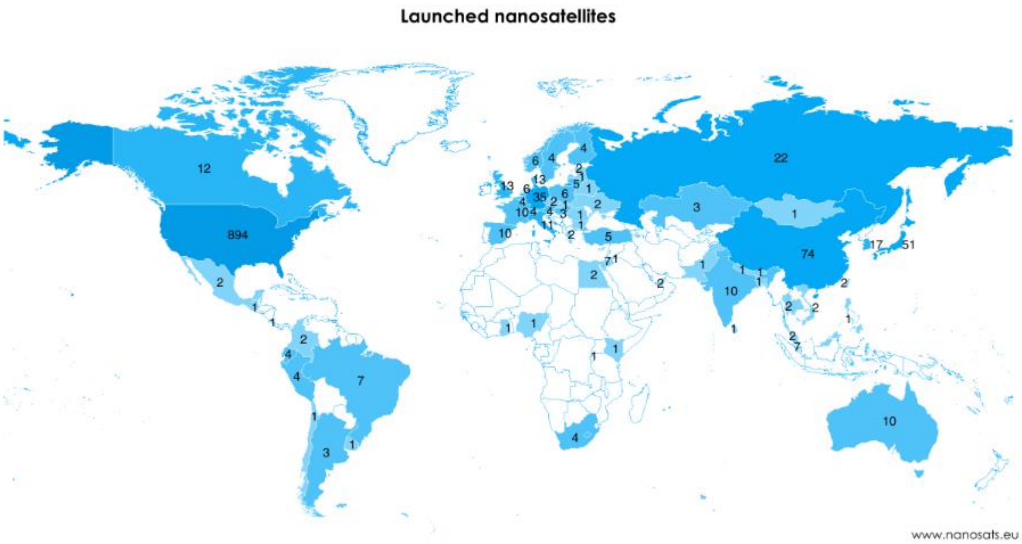

Figure 3: Number of CubeSat satellites sent by countries [7]

Figure 3 shows the number of satellites sent by countries. Currently, the United States takes the lead in the number of CubeSat senders.

Figure 4: The Nano Racks CubeSat Deployer deploying the SHARC satellite from the ISS [8]

The term "Cube Satellite" refers to the satellites in the form of cubes with a size of 10x10x10cm and a wet mass (weight including fuel) not more than 1kg. These standard dimensions are considered as one unit and denoted by 1U. Cube satellites are often produced as 2U (10x10x20cm), 3U (10x10x30cm). These standard dimensions are only limited areas of the satellite inside the rocket carrying it into orbit. After leaving the rocket, the satellite can change its dimensions, for instance, the folding solar panels can be opened to have a larger surface area. Figure 4 represented one of the sample that the CubeSat deployment from International Space Station (ISS).

1.2 Attitude Determination and Control System

Basically, determining the orientation in satellites is obtained by using the measurements obtained from the orientation sensors in orientation determination algorithms together with mathematical models. The sensitivity of the obtained orientation changes depending on the measurement sensitivity of the orientation sensors and the algorithm used. Magnetometer, Sun sensor, and horizon sensor are the orientation sensors frequently used in satellites today. If the orientation of a satellite becomes uncertain, then it may lose its communication with the ground station or it cannot benefit from solar energy with the desired efficiency, in which case it may not be controlled again. The damage that may occur can result in the loss of complete control of the satellite. Frequently used reference vectors are specific vectors that are directed at the sun, the center of the earth, a known star, or the earth's magnetic field. Orientation refers to the relationship between two different coordinate frames. The orientation in satellites refers to the relationship between the satellite body coordinate frame and the coordinate frame selected as a reference [9].

1.2.1 Sensors

The satellite must be combined with a system that can support triaxial orientation detection in sensors selected for direction determination. There should be a system with high accuracy for each axis. There are two main sensors in determining the orientation of satellites. The first of these is the inertia detectors and the other is the reference detectors. It is imperative for all sensors to have 3 axis information for calculations in the space plane. In order to ensure the correctness of the orientation, data is continuously updated with the earth's magnetic field, its angle with the sun or the sensor positioned according to the stars. The placement of the sensors of the satellites is important for precise referencing and precise positioning and orientation are important for all functions of the satellite to work.

In this study, 3 axis magnetometer and 3 axis acceleration sensors are used for referencing. The magnetometer is used to refer to the satellite, while the acceleration sensor is used to detect the satellite's inertia. If the sensors are classified according to their pros and cons, a selection can be made according to the selection of the systems to be used. For instance, when we classify it according to the degree of accuracy, gyroscope for inertia and star detection systems for referencing are the leading ones. It is the best sensor magnetometer that is efficient and cost effective at low altitude for reference. [10].

1.2.1.1 Sun Sensor

Sun sensors are the most commonly used sensor type in satellites. As they are used in satellite orientation systems, they are also used for different functions such as protecting devices affected by solar rays on the satellite and directing solar panels. Solar sensors are basically devices that detect the orientation of the Sun relative to the satellite (the Sun vector) in two axes [11]. The main reason why these sensors are widely used in satellites are; the sensor design and sensor data are easy to use because the Sun is far enough to be considered a point source for Earth-orbiting satellites and is bright enough.

1.2.1.2 Star Tracker

Star trackers are sensors that detect the position vectors of stars in space within the satellite body coordinate frame and compare these measurements with the positions of the stars in the reference coordinate frame. Star sensors are sensors that detect orientation with the highest accuracy (~ 1 arc second) compared to other orientation sensors. However, their high cost, large size, high power consumption, and the necessity of special algorithms for their operation are also negative features [11].

1.2.1.3 Magnetometer

Magnetometers are devices that measure the Earth source magnetic field vector in three dimensions in the body coordinate frame. Due to their light weight, lack of moving parts, low power consumption, and low cost, they are one of the most widely used sensors in satellites. The ability to operate in situations where other measuring devices are inoperative, such as a solar eclipse, almost necessitates their use on Earth-orbiting satellites. However, the orientation information to be obtained from the magnetometer is obtained in two axes since it is not possible to determine the orientation angle around the magnetic field vector. The use of magnetometers is limited to low-orbit satellites because the intensity of the magnetic field vector emitted from the Earth decreases with the cube of the distance. Figure 5 show that one of the sample Earth’s magnetic field model. Borb is the vector direction of the earth's magnetic field lines.

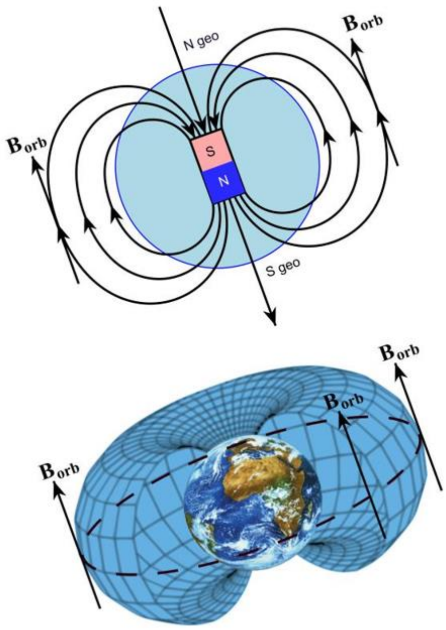

Figure 5: Single dipole model of the Earth’s magnetic Field [12]

1.2.1.4 Accelerometer

Accelerometers are devices that measure the acceleration applied to a mass. It is not necessary to know the coordinate acceleration (reference acceleration) in the measurement of the applied acceleration. Instead, the accelerometer looks at the applied forces on the reference axis due to the mass within the test mass. For instance, while the value of the accelerometer on a flat surface in a region close to sea level on the earth would be 9.81 m / s², the value it would show on a free falling object or in empty space would be 0 m / s². It is determined by processing the data received from the acceleration sensor, especially in determining the movements of the satellite. The rotation direction of the satellite and its change in speed are determined.

1.2.1.5 Gyroscope

Gyros operating at all points in orbits can be placed anywhere inside the spacecraft. However, they are affected by drifts. Therefore, it is preferred to be used with other sensors to ensure the full accuracy of CubeSat angular velocity.

1.2.2 Actuators

Actuators on the satellite have a mechanism that generates control torque for directional control systems. Torque generators are located in the satellite and allow the satellite to rotate in all three axes. In order to physically change the orientation of a satellite, a force effect must be created. There are two different methods, active and passive, to create this effect in the space environment. Active actuators to be applied to move the satellite in 3 axes need an energy source and consume energy. The most commonly used actuators are thrusters, magnetic torque coils and reaction wheels. With passive control systems, they use environmental energies to keep the direction of the spacecraft stable, for example gravity gradient bar and solar winds are the most common examples. The next step after determining the orientation target and current position of the spacecraft with sensors is how to direct it towards the target with a force. As mentioned in the previous chapters of a satellite, the orientation needs to be changed in order to dampen distortion torques from the outside or to take images with a camera. In this study, the force was created by controlling the effects of the magnetic field of the earth and the magnetic torque to be created by the current passing through the copper wire for active orientation control, and the placement of the actuators was made with a mechanism that would have the least area for a satellite. Commonly used actuators will be briefly mentioned below.

1.2.2.1 *Magnetic Torquer*

Magnetic torque generators are one of the easiest and cheapest methods to generate force by taking advantage of the Earth's magnetic field in direction determination systems. The torque to be applied is both controlled by current and is proportional to the distance to the Earth's magnetic field strengths. They are frequently preferred in active control methods.

To give an example of the systems used, if we look at the commercial ready-made products that are currently sold with CubeSat materials, the magnetorquer used in Figure 6 is the ISIS magnetorquer board (iMTQ) is a PCB based 3-axis magnetic system. It is designed to provide maximum flexibility in placing actuators and magnetometer in a CubeSat structure [**13**].

Figure 6: Three actuators; two torque rods and one air core torque. [13]

1.2.2.2 *Reaction Wheel*

It can move the spacecraft with the force generated by using angular momentum for 3-axis orientation control. For 3-axis control, reaction wheels should be mounted in at least three directions, with extra wheels providing additional redundancy to the attitude control system. An additional configuration of the wheel assembly axis or three-axis can occur through a tetrahedral spare wheel carried in addition to the configuration. Changes in speed (in both directions) are electronically controlled by the computer.

1.2.2.3 Thruster

Thrusters are the least used active elements in ADCS due to their fuel/gas needs, and they are expensive systems because of their many mechanical systems. However, it is especially preferred in large satellites because the impulse forces they generate are greater than other systems. Response time and accuracy are high precision [14].

CHAPTER II

PURPOSE OF THE STUDY

The aim of this study is to use the minimum space inside the satellite for the ADCS system of a 3U cube satellite operating in a low earth orbit. The system operation firstly determines the satellite's position and orientation movements from the sensors data, and then moves the magnetorquer forces to appropriate positions. The purpose of this study is to design and tested that is the CubeSat body effect of the torque generated by the magnetic field. It is the force created by the magnetorquer obtained with the coil wrapped in the body frame, which is theoretically calculated and leads the satellite design work that is planned to be realized in the future.

Small satellites contain useful payloads for one or more specialized tasks. However, the main system blocks must be well defined in every satellite. Examples of these functions are basic tasks such as attitude determination, attitude control, and the satellite's viewing system of the earth or the solar panels to harvest the energy from the Sun. After the satellite deployment is done, first it attempts to stabilize itself in the desired orientation in the orbit, otherwise, it can spin around itself and this situation may carry on permanently. First of all, the CubeSat body mainboard should decide the orientation that it needs to take. Data analysis is done about the correct position and error rate. In our study, it is primarily determined by movements made by the orbit analysis in CubeSat sensors and the moment that is generated to perform inverse action to damp the rotational movement. Magnetorquer is used to create these moments. Magnetorquer are obtained by creating an electromagnetic field through current in coils placed in multiple axes. Additionally, they are perpendicular to the magnetic field so that the desired damping forces or target locking occurs. While CubeSat rotates around the center of gravity, its movement to dampen its rotation is provided by 12 different coil loops wrapped around the CubeSat body. Here, the moment of each coil is affected by multiple factors; the distance from the center of the coil and the earth, the magnetic field of electric current that produce the force, the number of coil turns, the wire thickness, and the rectangular winding area. The direction of the electric current determines the vector direction of the moment and can be reversed in the H-bridge driver [15-16].

The most important advantage of the system is the creation of forces that are perpendicular to the magnetic field using 0.15mm-thick coils wrapped in the CubeSat body frame skeleton; which are already there to provide stiffness and strength. Through this mechanical reuse advantage, the CubeSat frame is strengthened and more space for other payload systems is gained. Crosslines are especially used for the coil winding around the CubeSat body frame. This increases the effect of forces on turns. CubeSat body frame is divided into four equal parts and then combined into two identical parts. Two windings were made for each of the four. After that, the two parts are externally combined with the other two winding turns, and finally, integration is done. These directional forces create a resultant equivalent force in the system. For these moments in order to stop at the targeted orientation, moment directions are decided using the gain coefficients from the preset lookup table. This way, the transaction processing load is reduced significantly on the microcontroller.

The current intensity level is provided by control algorithms. The decision-making data here is determined by the algorithms processing the data coming using the magnetometer, accelerometer, and gyroscope.

In the test setup here, only the case in orbit is analyzed. When CubeSat is taken into the first rocket, it has mechanical dimensions of perfect 3U standards. Also, it is assumed that it makes 45 degrees' angle movement with a mid-plane moving mechanism to increase the efficiency of the solar system with tilted panels.

The information received from the sensors is crosslinked in each direction and digested into controls for 12 different coils that are driven independently [17].

For 3 axis stabilization, each axis is controlled to be highly efficient with a simple PID algorithm. Firstly, the difference between the angle that is targeted to be reached and the fixed body position is determined and the error signal is dynamically scaled through the lookup table before igniting the set of appropriate coils. PID algorithms that provide control with different PID coefficients are designed for all three axes [18].

2.1 CubeSat System Structural Design

Many designs are used by placing the surface in the third axis of the magnetorquer on rod or body. In these studies, when the rod is added, it covers a considerable area in CubeSat. There are square-shaped coil designs placed on CubeSat inner surfaces and they are preferred to be in 3 axes as presented in [19].

In this study, coil wires were wrapped inside the body frame as in Figure 7 to reach the required field strength. The structural architecture is quite distinct. When the solar panels are opened after leaving the rocket in the orbit, the moving mechanism in the middle rotates the two halves by 45 degrees with respect to each other. The coils are wrapped cross body, and this has advantages. One of the advantages is that it creates a multipoint simultaneous force injection mechanism for better traction. The structure used in the experimental prototype shown in Figure 7 is PLA material from a 3D printer. In order to wrap the coils, channels were opened in the CubeSat body. Coils were formed from wires of 80 turns and 0.15 mm in diameter.

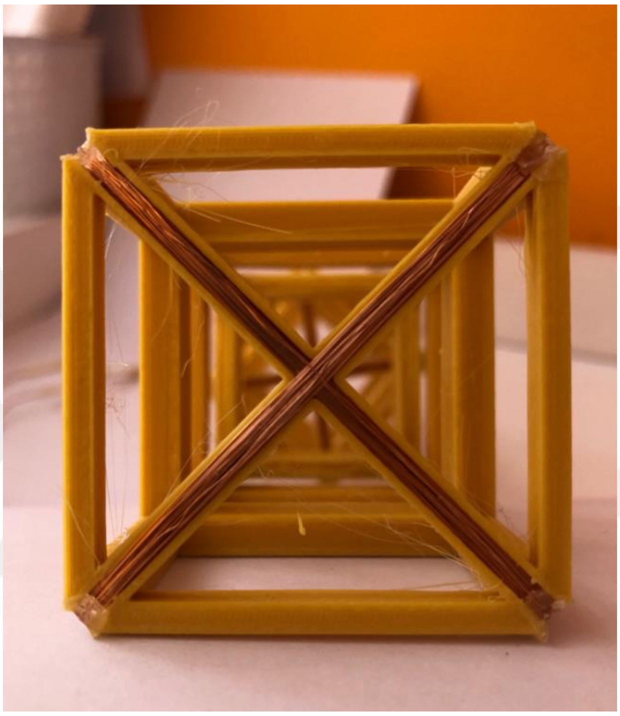

Figure 7: Photograph of magnetorquer coil-embedded body

2.1.1 Installation of the Satellite's Body Frame Coil Winding

The satellite was firstly divided into 4 parts and produced with a 3D printer, and while designing, channels were created where the coils were coiled. In Figure 8, there is a photograph of a part of a CubeSat body divided into 4 parts.

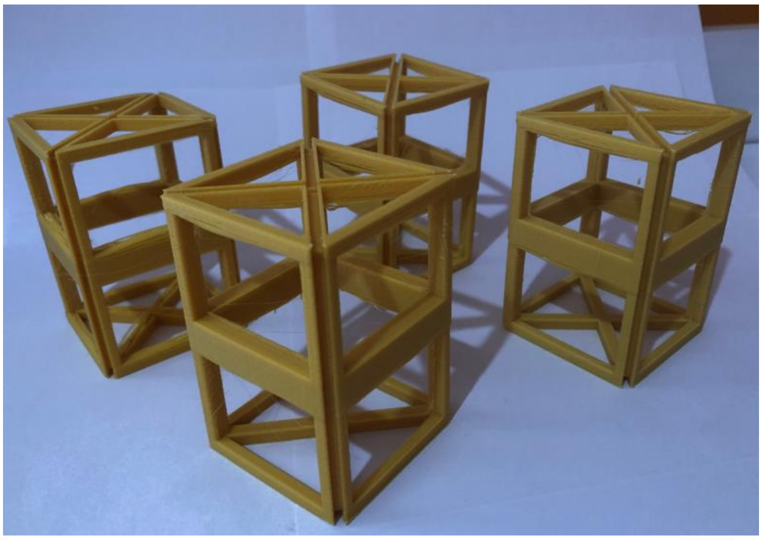

Figure 8: Individually produced body frame parts

Coil winding was carried out in these produced parts in crosswise directions. The windings of the coil wires are shown in Figure 9.

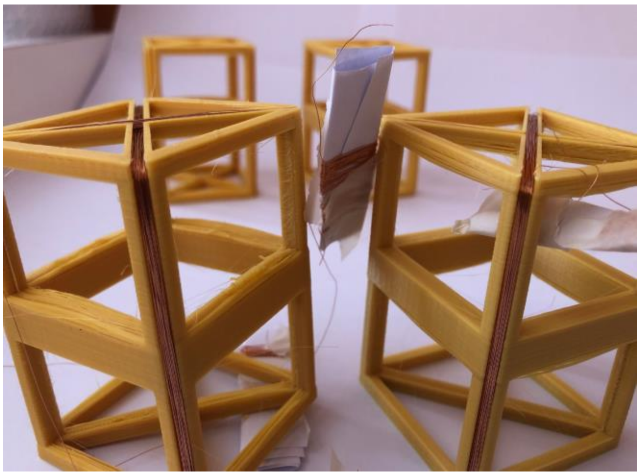

Figure 9: Windings of coil wires

After the parts were wrapped with wire, the body frames were combined for the first and second stage, which would form half of the CubeSat, and then the large coil wire was wrapped to have a larger area. Figure 10 show a body frame combined. When these two body parts are combined, the total length becomes 150 mm.

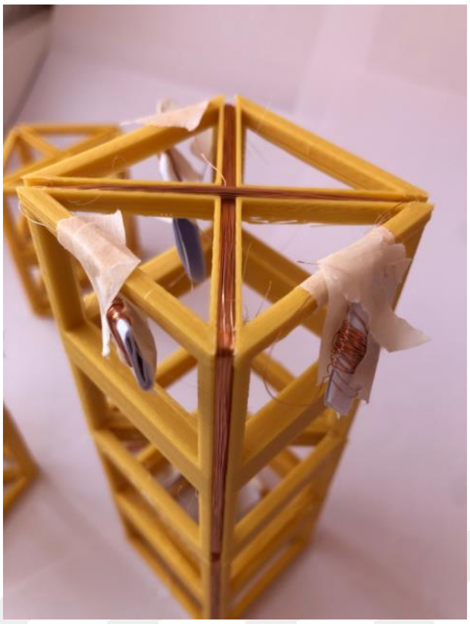

Figure 10: Coil winding top view

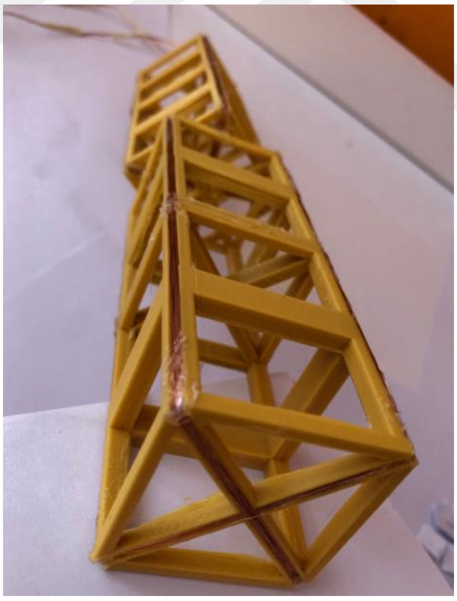

Figure 11: Combined view of all parts

Figure 11 shows the combined view of the whole body. Novel to our approach is that the CubeSat body is rotated 45 degrees from its midpoint. On this basis, the CubeSat is designed for the movement that will occur when it comes out of the rocket in space, but this study includes an analysis of its state after leaving the rocket. For this reason, the system is 45 degrees offset from its midpoint.

2.1.2 Magnetorquer Coil Design

Magnetorquer are created using electromagnetic coils to perform control, dissembling, and stabilization in satellite systems. Using the earth's electromagnetic field, high levels of torque can be achieved [20].

Magnetorquer are light, reliable, and energy-efficient. Unlike thruster, they do not need propellant that might be depleted prior to the lifetime of the CubeSat. Magnetorquer on the other hand can work indefinitely, as long as there is theoretically enough power to overcome the resistive load of the coils. Sunlight in earth orbit is a renewable source of energy that is used for solar panels.

Comparing to momentum wheels and control moment gyroscope, the absence of moving parts is significantly adding higher reliability because of none of the associated mechanical friction and wear [21].

Figure 12 shows that CubeSat has just coils wrapped on the body frame. The magnetorquer designed in this study is wrapped around a 7,07cm x 7.5 cm cubic piece with a coil wire of 80 turns and 0.15 mm in diameter.

These 7.5 cm cubes, consisting of 4 parts, are wrapped 80 turns with 0.15mm thick wire. Coil for the body frame consisting of 15cm x 5cm x 5cm to be combined with two-stage. In Table 1, the number of turns, thickness, and area dimensions of all windings are given.

Table 2: Dimension Parameters of Magnetorquer Coil

Coil Name 1 stage	F2,F3,F5,F6	F1,F4
Coil Name 2 stage	F9,F10,F11,F12	F7,F8
Number of Turns	80	80
Bare wire diameter	0.15mm	0.15mm
Cross Sectioan Area	0.005303 m2	0.00975 m2
Apply Voltage	10 V	10 V

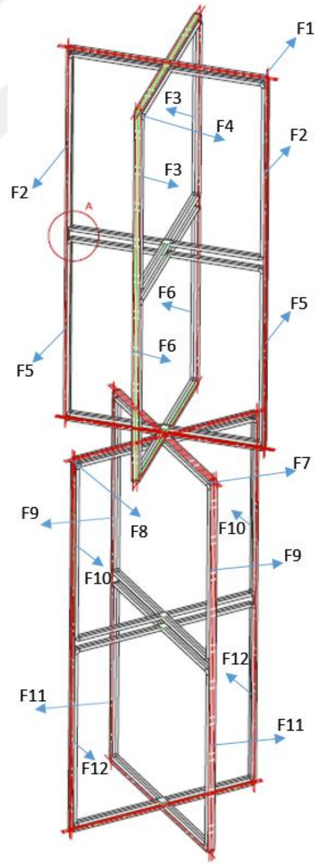

Figure 12: Coil windings and forces are shown in vector.

Some situations are considered hypothetical for dynamic modeling of a cube satellite. In one of these cases, the satellite is supposed to behave like a completely solid body. The spacecraft is assumed to act as a point mass model for orbital dynamics. The applied torque changes depending on the angular momentum and is accepted according to the Newton-Euler formula. The dynamic model with these assumptions is given Equation 1 [22-23]. I is the moment of inertia W_{bi}^{b} is the angular velocity of the body frame relative to the inertial frame in the body frame.

$$T^{b} = I\dot{W}_{bi}^{b} + W_{bi}^{b} \times \left(IW_{bi}^{b}\right) \tag{1}$$

Magnetic torquers are selected as actuators for stabilization mode, T^{b} is the torquers acting on the satellite in body frame given Equation 2. It is equal to the sum of the gravitational torque on the satellite body, the torque applied by the magnetic torquer and total disturbance torques.

$$T^{b} = \dot{T}_{grav}^{b} + T_{mag}^{b} + T_{dis}^{b} \tag{2}$$

When the Euler angles are Roll ϕ, Pitch θ, and Yaw ψ, the relationship between Cubesat body angular velocity and Euler angle rates is shown in Equation 3.

$$\begin{vmatrix} Wx \\ Wy \\ Wz \end{vmatrix} = \begin{vmatrix} \phi + W0\psi \\ \theta - W0 \\ \psi - W0\phi \end{vmatrix} \tag{3}$$

There are gravitational gradient torques that use the small Euler angle approach and take the main axes as the reference axis. [24]. Equation 4 shows that T_{gravx}, T_{gravy}, and T_{gravz}, are the gravity torque axes. They are explained in [25] reference.

$$\begin{vmatrix} T_{gravx} \\ T_{gravy} \\ T_{gravz} \end{vmatrix} = \begin{vmatrix} 3W_0^2(I_z - I_y)\psi \\ 3W_0^2(I_z - I_x)\theta \\ 0 \end{vmatrix} \tag{4}$$

Magnetic torquers calculations for this system are done separately for each coil and torques are added in vectors. The 12 coils are controlled independently and the vector distance is taken according to the x, y, z coordinates, which are accepted as a reference.

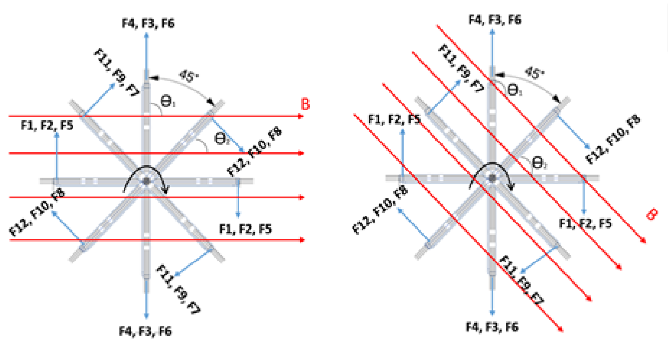

(A) (B)

Figure 13: Coil design top view

Figure 13 shows the top view of the torques generated by coil turns which has a width as given in Figure 13.A and height as given in Figure 13. B Magnetic field is assumed to be uniform over the rectangular loop. The difference between Figure 13.A and Figure 13.B is that if the magnetic field changes the direction of the vector, the effect of which forces will change.

$$T_{mag}^{b} = \sum_{a=1}^{12} x_a * y_a * i_a * N_a * sin\theta_a \quad (5)$$

In the Equation 5, x_a and y_a represent the winding lengths i_a is current through the coils, Θ is the angle between coil and B that is the magnetic field of the earth N_a is the number of return coil windings [26].

Figure 13.A shows the magnetic field lines and the force directions of the torques that coils will generate. Directions of force depend on the direction of the current. The method contemplated here has been accepted for the realization of the yaw movement. The biggest advantage in this method is that the angle between the magnetic field and the coils are created in any case below 45 degrees of thrust. This way, more precise orientation can be achieved in any arbitrary position case.

Figure 13.B, when the orientation of the magnetic field changes, it can be seen which coils have more effective generated force. The change in figure 13.A and figure 13.B is entirely related to the $sin\theta_a$ of the equation given in formula 5.

2.1.2.1 Magnetorquer advantages and disadvantages

There are a lot of distinct advantages that using a magnetorquer ensures over alternative control systems. Unlike other active actuators that need consumable materials, such as thrusters, they can in theory work indefinitely as long as sufficient power is available to match the resistive load of the coils. The absence of moving parts makes them significantly more reliable than using momentum wheels and control moment gyroscopes. Magnetorquers consume little power and occupy less volume than alternative control systems.

Despite their unique benefits, there are some disadvantages to using magnetorquers alone to manipulate and control satellite attitude. The torques that can be provided are very limited and only serve to accelerate or decelerate the change in a spacecraft's attitude by minute amounts. It may be impossible to control attitude in all three axes, even when the full collection of three torquers are used because the torque can be generated only perpendicular to the Earth's magnetic field vector. Their dependency on the Earth's magnetic field makes the use of magnetorquers difficult beyond the Low Earth Orbit (LEO). Despite these problems, magnetorquers remain one of the most successful and popular options for attitude control systems.

CHAPTER III

ATTITUDE CONTROL SYSTEM OVERVIEW

For the general definition of Attitude control system, some definitions will be made in this section. First of all, the system under study will be defined and the electronic circuit card will be introduced, and then the algorithms used in software development will be used.

3.1 System Description

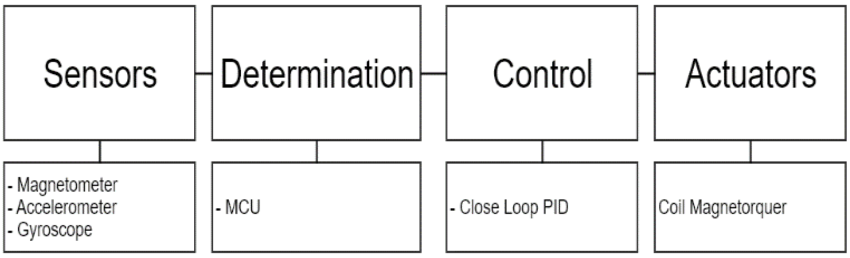

Figure 14: Software Flow Diagram

In the proposed CubeSat ADCS system, the motion is analyzed in 3 axes and axial movements of the CubeSat body are determined. Figure 14 shows the general algorithm diagram. The difference between the targets set in the central system and the current position is determined as an error in the control system. 45-degree rotation in the moving system does not affect the closed-loop system. The factor that will determine the directions of the moment that will occur here is related to the angle between target and moment. The lookup table is used to reduce processing power in the software. Utilizing a lookup table, the difference between targeted position and current position is observed and the directions of the forces are determined according to this difference. The intensity of the moment is directly proportional to the currents passed through the coils, and the factor of the forces here is determined by the close loop algorithm with the data from the accelerometer. The difference between target and data from the sensor data will be the variable we consider to be an error. To decrease this value, the magnitude of the torque to be created was changed with the PWM signal to be applied to the coils.

3.2 Hardware

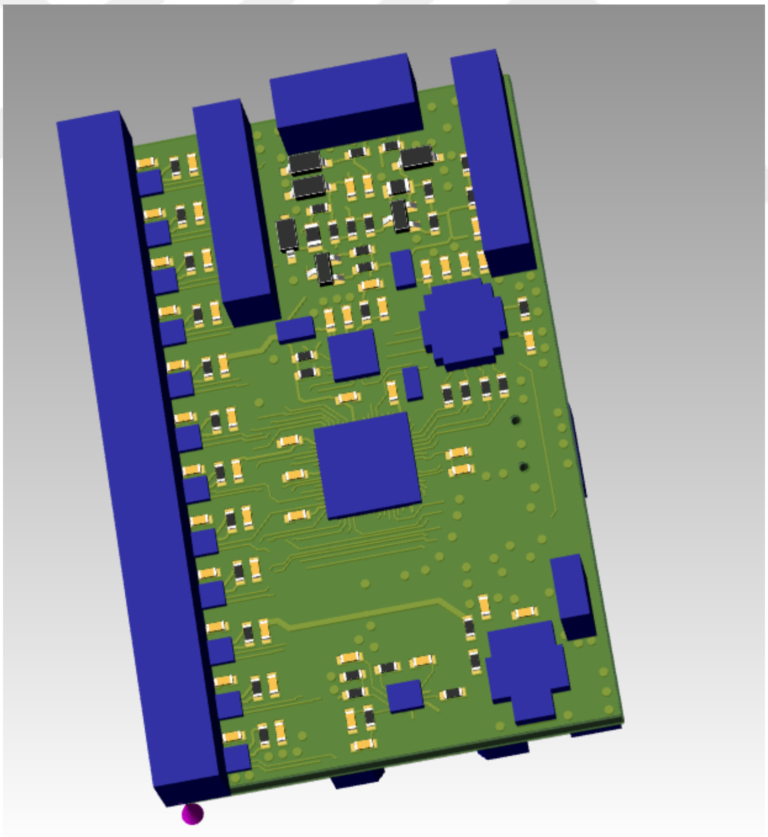

Figure 15: Photograph of the controller mainboard 3D view.

The circuits that are required for the entire electronic system are combined in a single board. This mainboard includes all the movement sensors, such as gyroscope, magnetometer, accelerometer as well as power and processing subsystems such as H-Bridge divers, LDOs, Boost Convertors, Microcontroller with PWM drive capability. Printed circuit board design was realized in 4 layers which are made of FR-4. There are 12 optional bridge coil driver outputs. The desired voltage for magnetorquer is increased by the step-up converter and was obtained on the board. The main system supply is a 3.7V Li-Ion battery pack while the drive supply for the coils is set to be 10V to yield large currents in case needed. Figure 15 is show that 3D view of mainboard layout design for last control before ordering PCB layout and checking electronic part placement. An overview of the mainboard having all components is shown in Figure 16.

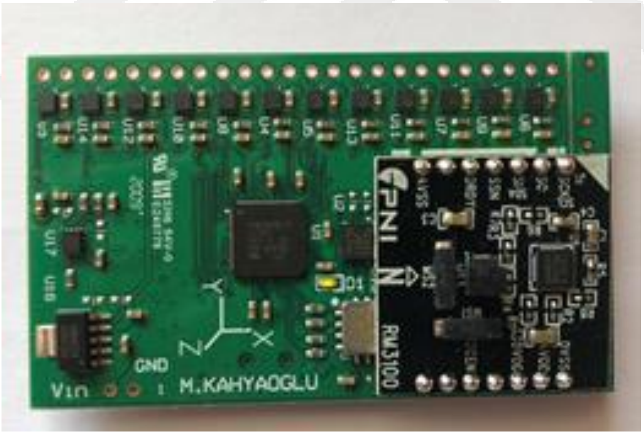

Figure 16: Photograph of the controller mainboard module.

Data was sent with a wireless communication module to display data for testing and understand situations during development. Acting like a computer ground station, it visualized the movements of the satellite on the screen, and at the same time it graphed all the information. More detailed information about the test is given in the sections below.

3.2.1 Sensors

Acceleration sensor, gyroscope, magnetometer sensors were used to determine the position of a satellite and orientation movements in determining the orientation. Brief information and circuit diagrams about the sensors used are explained in the following sections. In addition, all the sensors used were made with commercially available sensors. The sensory data reading frequency is 1 kHz.

3.2.2 Magnetometer RM3100

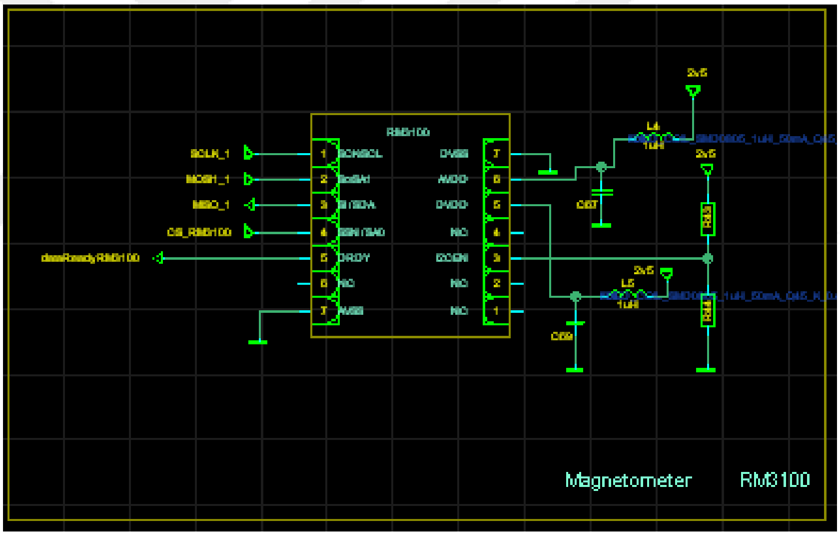

Figure 17: Magnetometer schematic circuit

A magnetic field sensor is used to measure the magnetic flux density. Magnetic flux density levels in 3 axes were measured according to the position of the sensor of the satellite with the data received from the RM3100 sensor placed in the satellite. In addition to being very sensitive, magnetic sensors are cheap and light in weight. The accuracy of magnetic meters depends on the effects of many electromagnetic disturbances in satellite subsystems and needs to be calibrated. The fact that the Earth's magnetic field model is not correct also reduces the accuracy of the orientation data obtained from magnetic meters. Figure 17 shows the circuit diagram of the magnetometer breakout board and Figure 18 represent to RM3100 evaluation board pinout information.

RM3100 magnetometers of PNI Company were used as magnetic sensors in this study. This was our choice because of its high resolution and low power consumption and sensitivity to electrical and magnetic noise. Measurements were made at room temperature and observed deviation. There are two coils on the RM3100 test board. With X, Y sensor coils and Z axis coils, PNI's MagI2C ASIC controller is available [27].

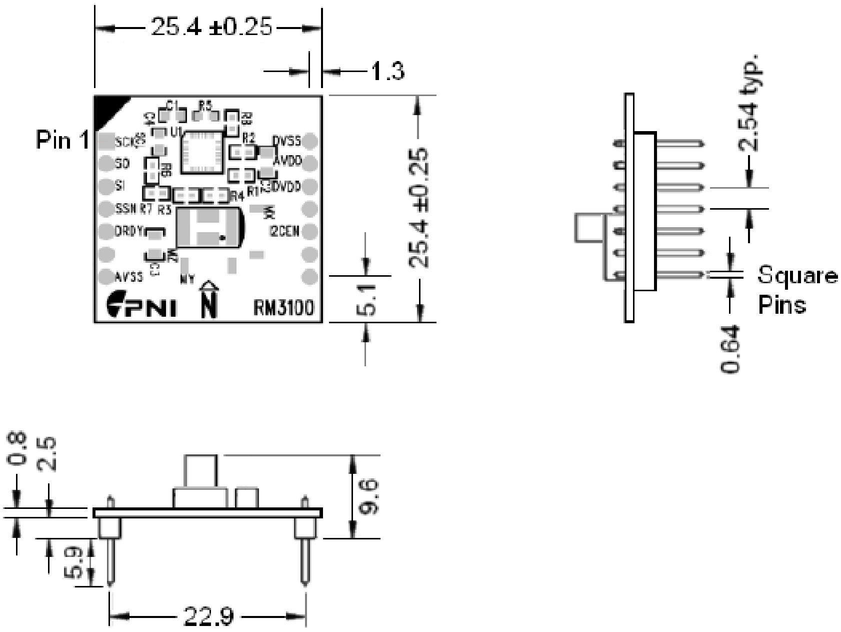

Figure 18: RM3100 Evaluation Board Mechanical Drawing

3.2.3 Gyroscope I3G4250D

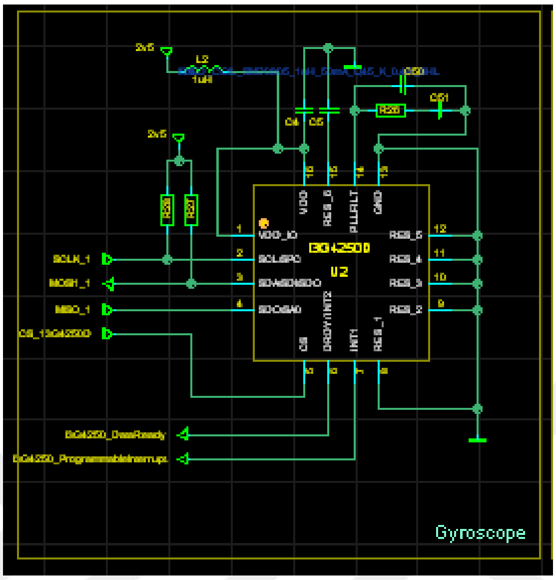

Figure 19: Gyroscope schematic circuit

A gyroscope is used to measure the angular acceleration of a satellite in 3 axes. I3G4250D was used for this study. It is a low power 3-axis sensor. Figure 19 and Figure 20 gyroscope schema circuit is shown.

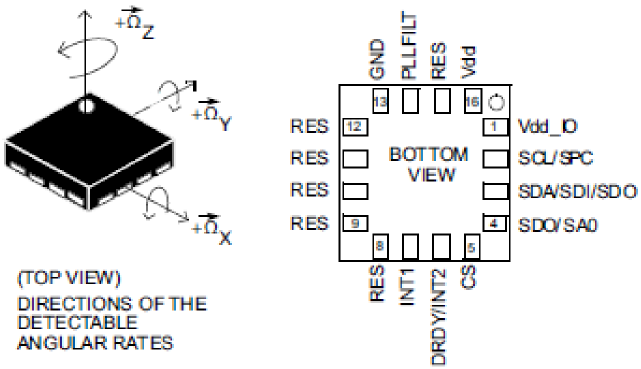

Figure 20: Pin output and view of axis [28]

3.2.4 Accelerometer ADXL356

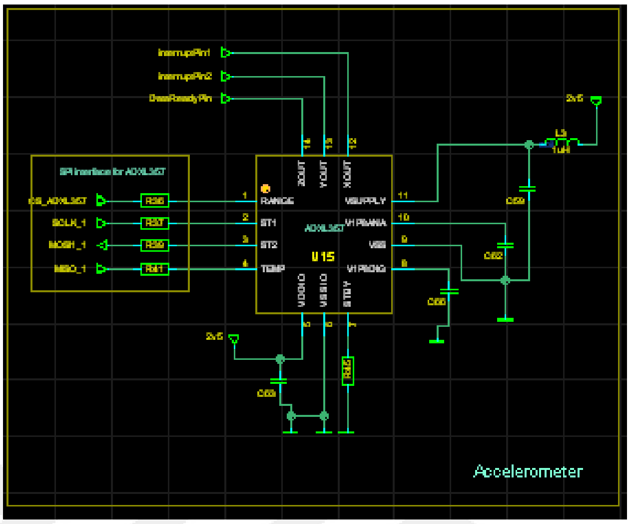

Figure 21: Accelerometer circuit diagram

ADXL357 sensor integration was used to determine the directional movements accelerated by the satellite. Data are the communication link between the MCU and the sensor using the SPI communication infrastructure. Figure 21 and Figure 22 show that pin and schematic circuit diagram.

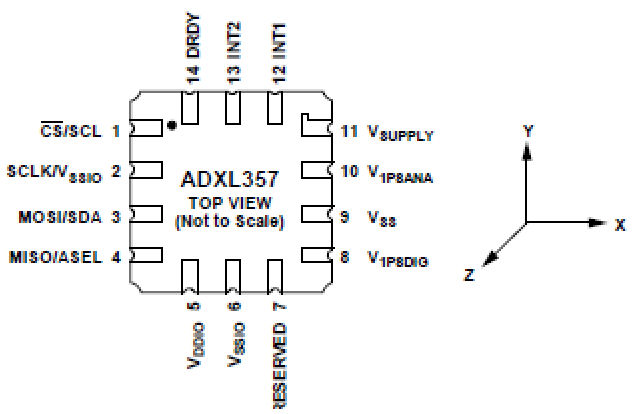

Figure 22: ADXL357 Pin configuration [29]

3.2.5 Coil Driver DRV8838

The DRV8838 made by Texas Instruments was chosen as the coil driver. DRV8838 is a tiny H-bridge coil driver IC that can be used for bidirectional control of coil at 0 V to 11 V. It can supply up to about 1.7 A continuously and can tolerate peak currents up to 1.8 A for short durations, making it an ideal driver for coil driver that run on low voltages. Figure 23 gives an overview of the schematics. The coil driver controller is a low voltage driver. A first stage converts the input voltage to 3 Voltage to 11 voltage stable Figure 24 shows that boost converter circuits.

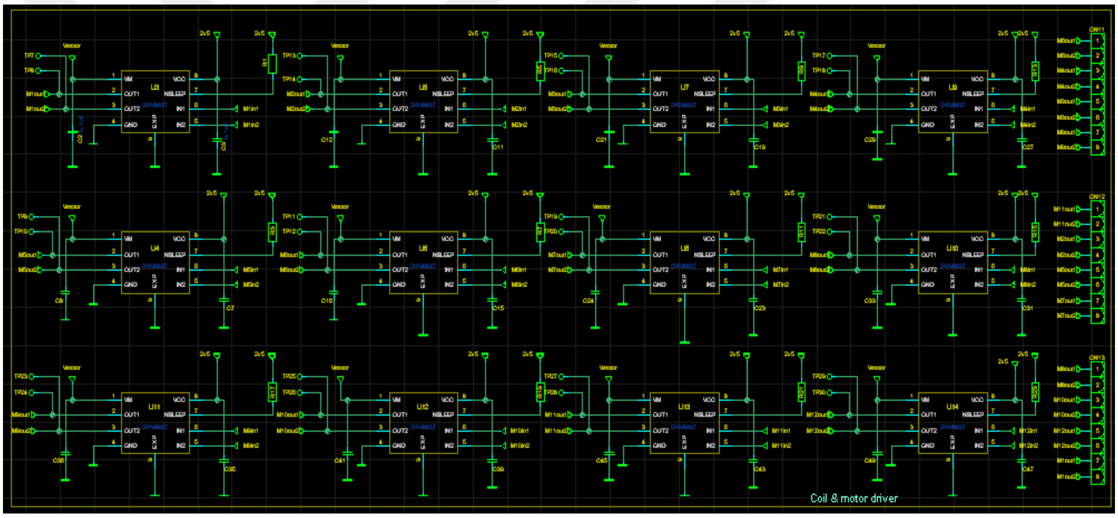

Figure 23: Schematics of the implemented coil driver.

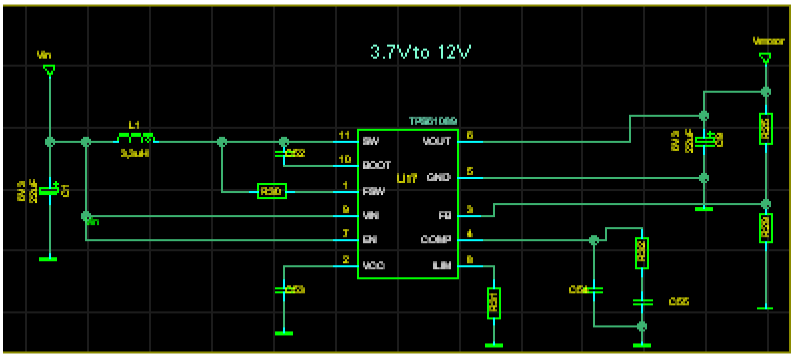

Figure 24: Boost converter circuit diagram

3.3 *Layout Design & Assembly*

After the circuit design, the layout design continued and the layout of the materials was designed by leaving a distance between the magnetic field sensor and the motor drivers in order not to affect each other electrically from noise. Layout work was done in Mentor Xpedition program. The PCB is designed as four layers, FR4, double-sided. Its dimensions are 39mm x 61mm. The pallet design is multiplexed in 6 pieces. For ease of assembly, the sensitive materials in the IC QFN sheath, SMD 603 package, etc. sheaths are arranged in a top layer. Figure 25 and Figure 26 are the layout view of the main board design.

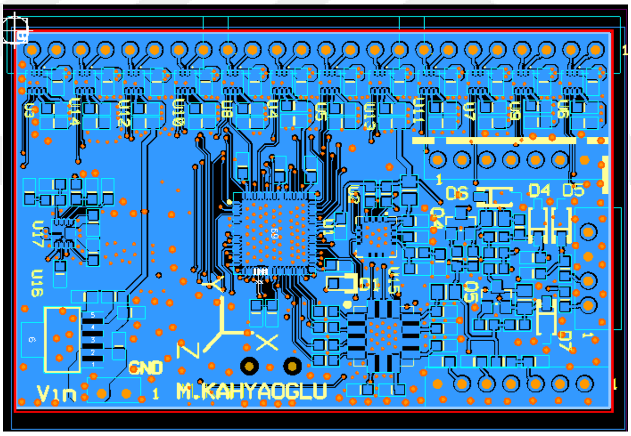

Figure 25: PCB Layout top surface

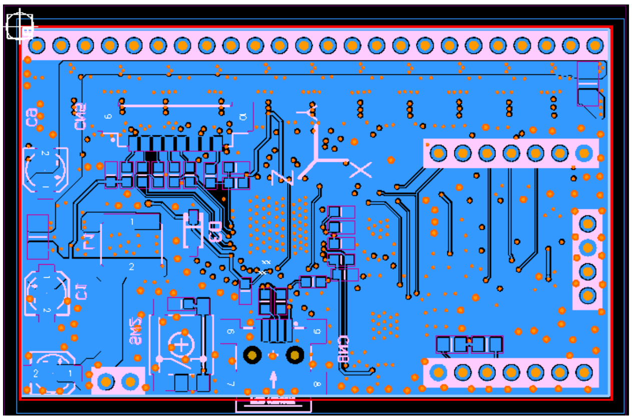

Figure 26: PCB Layout bottom surface

The design was made in accordance with the reflow method in order to be produced in auto assembly machines. PCB and top stencil were produced. After the materials were placed with auto assembly, the assembly of the materials on the card was completed with the baking process. Figure 27 and Figure 28 show that CubeSat mainboard when it was assembly electronic component.

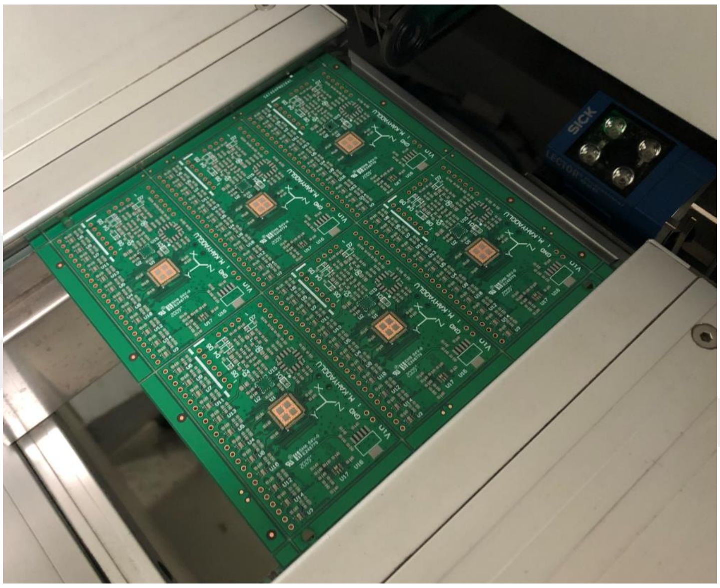

Figure 27: Auto assembly machine band

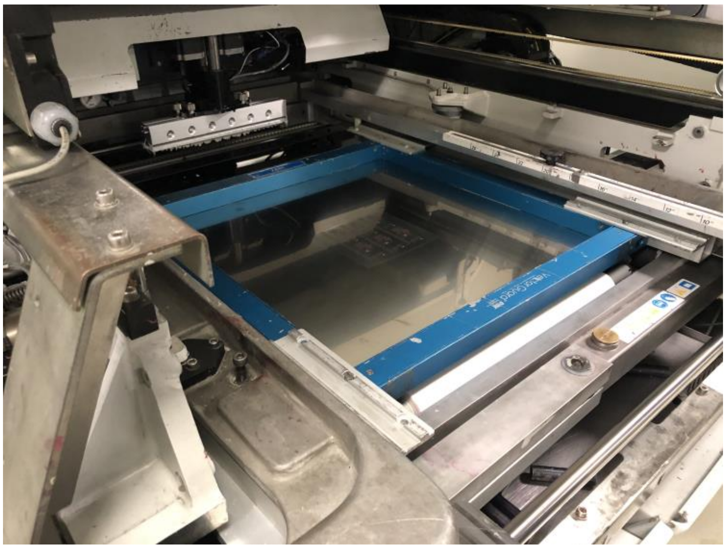

Figure 28: Soldering machine with stencil

CHAPTER IV

ATTITUDE CONTROL SOFTWARE ALGORITHM

CubeSat motion analysis is performed in three axes in the CubeSat Attitude Determination and Control System (ADCS) system. First, the current position of the body CubeSat determined direction and angular speed. The difference between the target and the current orientation, producing an error signal is fed to the central system. After sending an error signal to determine the current position and having feedforward PID algorithm is determined with a feedback process to enable the relevant aspects of proper torque wheel. Distance to the destination. B-Dot controller in all three axes as angular speed 5 °/ sec run until it drops below. Then, the closed-loop PID algorithm determines the effect of the angular torque margin.

The system, with its high-gain feedback PID action is forced to acquire a lock in the three axes. Every road feedback signal is also scaled proportionally and the other is forced to run with dynamic scaling appropriate for each branch of the possible locations. In this way, the designers were able to capture the overall stability of the system's status. Where in the basic additive, which correlates the operating level in the target drive torque from other relative directions coil is a multiple lookup tables that provide an excellent set of coefficients.

Six degree of freedom (DOF) motion tracking system for determining three axis gyroscope and ascending movements of the body frame CubeSat many applications that use three-axis accelerometers. Figure 29 shows a general block diagram of the algorithm.

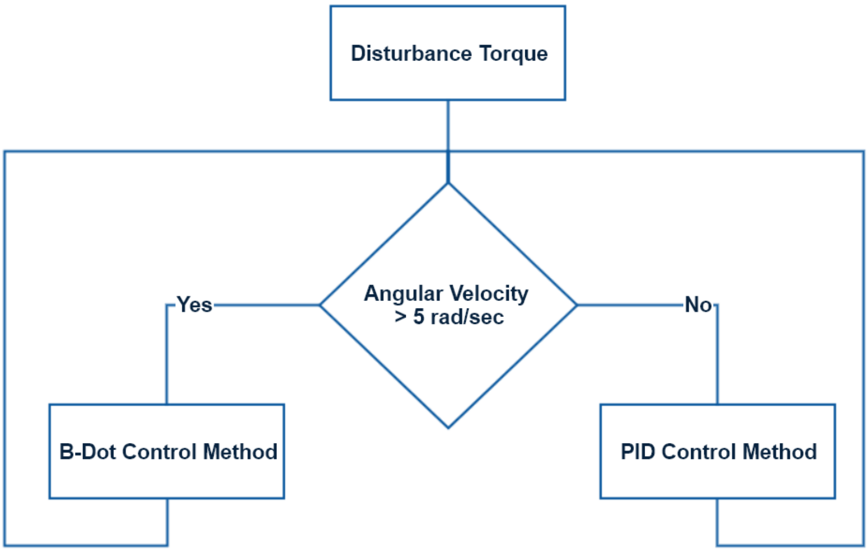

Figure 29: Software Flow Diagram

When the system is a low damped responded stable, external torque to change the route will affect the CubeSat continuous body. To overcome the undesirable torque ADCS active external noise effect is retained and absorbed in the required direction to provide the locking of the system.

4.1 B-Dot Control Method

After leaving a satellite rocket, for example, you must first break to reduce the angular momentum. This will create a force against the rotation direction and a constant rotation of the satellite is attenuated. Additionally, the B-Dot protocol is also valid in the case of increasing angular acceleration. The forces that will occur in the opposite direction are determined according to the values read from the gyroscope sensor. This study has activated the winding force in opposition to the direction of rotation of the satellite and angular conversion of 5 degrees/sec remain under PID algorithm when the target is locked into operation. Figure 30 represented B-Dot Control Method generic flow diagram.

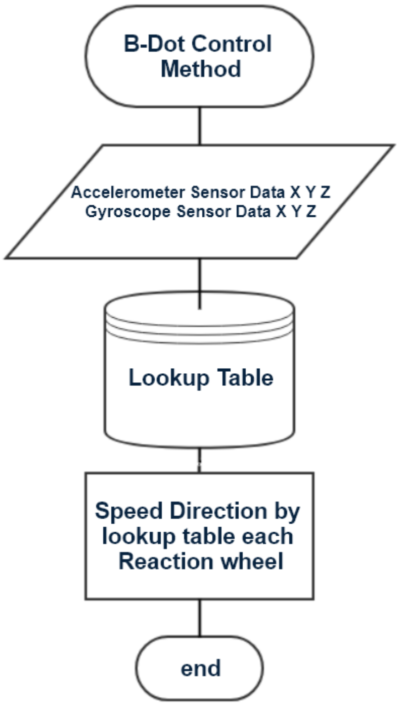

Figure 30: B-Dot Flow Diagram

4.2 PID Control Method

Proportional Derivative control law known as "PD" control law generates proportional law by adding a derivative term. The purpose of this differential terms, allowing more refined control is to provide the oscillating motion of proportional damping law. When the satellite approaches the desired target, precise movements must be made in order to stay stable. Therefore, when the target is approached, PID control is applied. [30].

Proportional integral derivative control laws or simply "PID", this integral term allows the elimination of the error accompanying permanent deformation as an external torque on the spacecraft.

In this study, first as Matlab / Simulink model analysis was performed and established a structure to interact with PID structure coefficients in three axes. The reason for this situation to affect the other axis of rotation of each axis movement and were made to improve the stability of the situation. PID parametric coefficients are found by iteration experimentally.

Different PID coefficients are determined for each axis. For the system to be more stable, a simplified mathematical model of the entire system is analyzed instead of the real mathematical model. The system has become stable under ideal simulation conditions. Figure 31 shows the Matlab/Simulink block diagram for the PID controller.

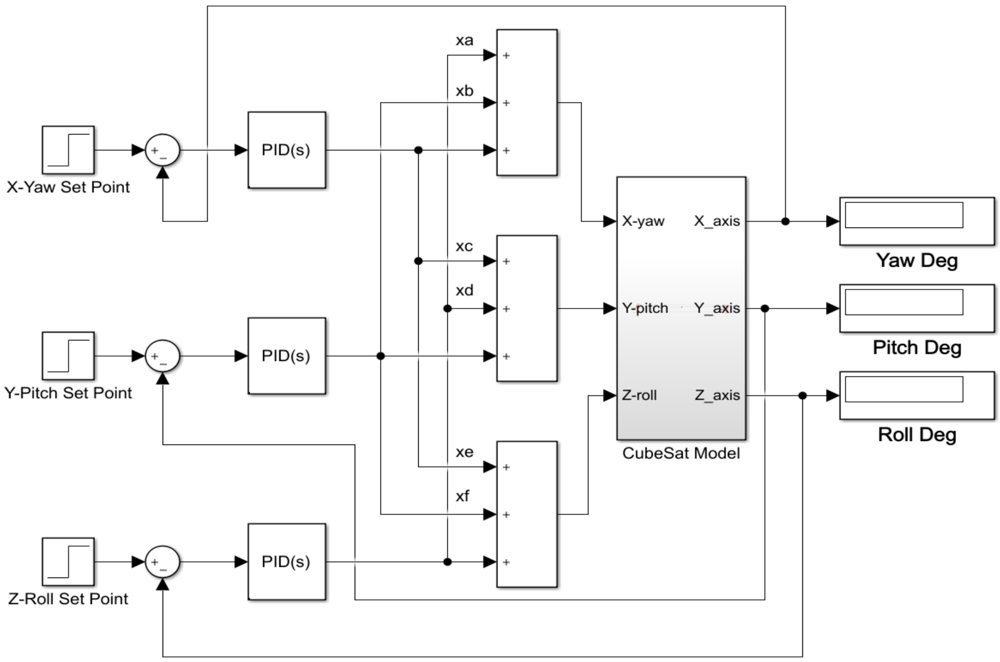

Figure 31: Simulink block diagram of CubeSat model with PID controller

The system is forced to attain lock in all three axes thanks to the feedback action with high PID gain. The feedback signal from each path is also proportionally scaled and forced into the other actuation branch with proper dynamic scaling for each of the possible positions. This way, the designers were able to capture the overall stability condition of the system. The key contribution here is a coefficient look-up table that provides a perfect set of coefficients relating the actuation level in the target coil to the torque in the other relative directions. Look-up table was designed according to the lookup table yaw movement and determined experimentally. Since, we can only make the YAW movement in the test setup. It was determined as "+" for clockwise rotations and "-" for counterclockwise rotations. "+" and "-" indicate the direction of the current passed through the coil. Figure 32 shows the direction of the Euler Angles.

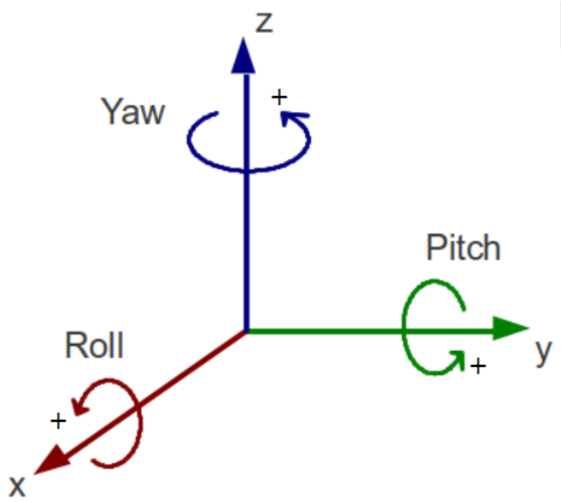

Figure 32: Direction of Euler Angels

CHAPTER V

EXPERIMENTAL RESULTS

The proposed CubeSat design and ADCS was experimentally tested using a custom made setup. The application was made on examining the effect of external disturbing torque application. The stability of the study was increased with repeated experiments for the analysis of the working state of the system. The operation of the ADCS system with the magnetic field torque generators generated from coil wires wrapped in a CubeSat body frame was tested.

5.1 Test Results

The test setup was carried out by hanging the system on a support point with a line such that it can turn freely around its axis in the laboratory environment. The test primarily shows the effect of the forces generated by visualizing the data from the sensors using Matlab program and activating the ADCS system. The test results of this setup are shown by visualizing the data in Matlab. An image of the test setup environment can be seen in Figure 33.

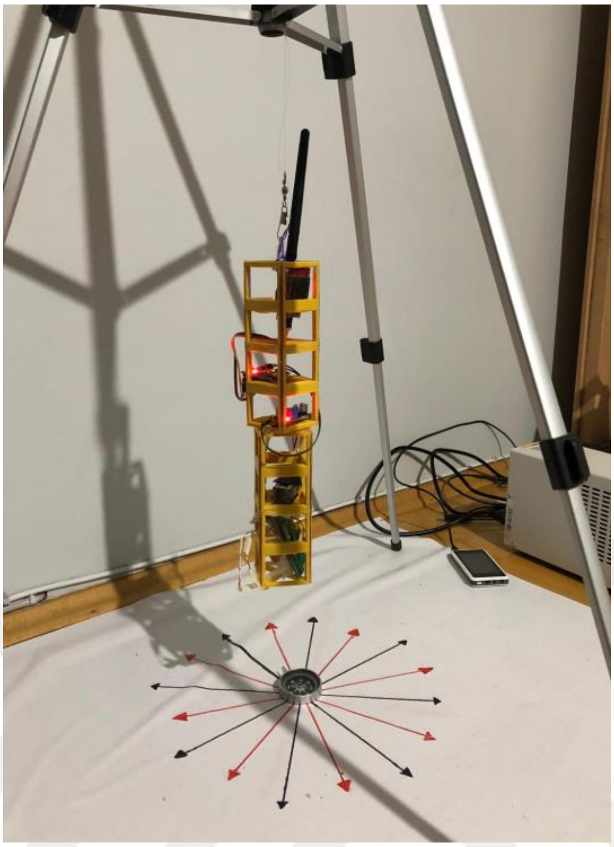

Figure 33: Photograph of the test setup

Software aided test setup is controlled by the main card, and only in the direction of the satellite routing information from the sensor transmits via wireless communication. The computer acts as a ground station and displays the values in the interface according to information from the satellites. Wireless communication is done with Xbee communication modules. The data received written for computer interface is monitored by the Processing language interface. The gyroscope and acceleration are designed as a 3-axis satellite. Data received from the computer test satellite has been marked as determined by ground stations.

The performance of the ADCS system depends on the coil windings in the frame of the satellite. As a result of this experiment, it showed how long the CubeSat body is stable when the ADCS system was active. Through the forces created against electromagnetic fields by the currents passed through the coil in a shorter period CubeSat body becomes stable and remains constant. As seen in the graphic, the disruptive force was applied to the cubes at different times and the system was re-stabilized by the counteraction of the ADCS.

The Eular angles of the CubeSat are taken to be [-360 360] deg about all the three-axis which is called X-yaw, Y- pitch, Z- roll.

The graphic shown in Figure 34, Figure 35, and Figure 36 shows yaw pitch and roll movement angles of the CubeSat. Figure 37 represented all axis movement angels of the CubeSat. In the figures below, straight lines are seen instantaneously, these lines are unwanted noise signals that occur during sensor reading.

In the graphs, the values that rise suddenly while in a stationary state show distorting movements applied externally.

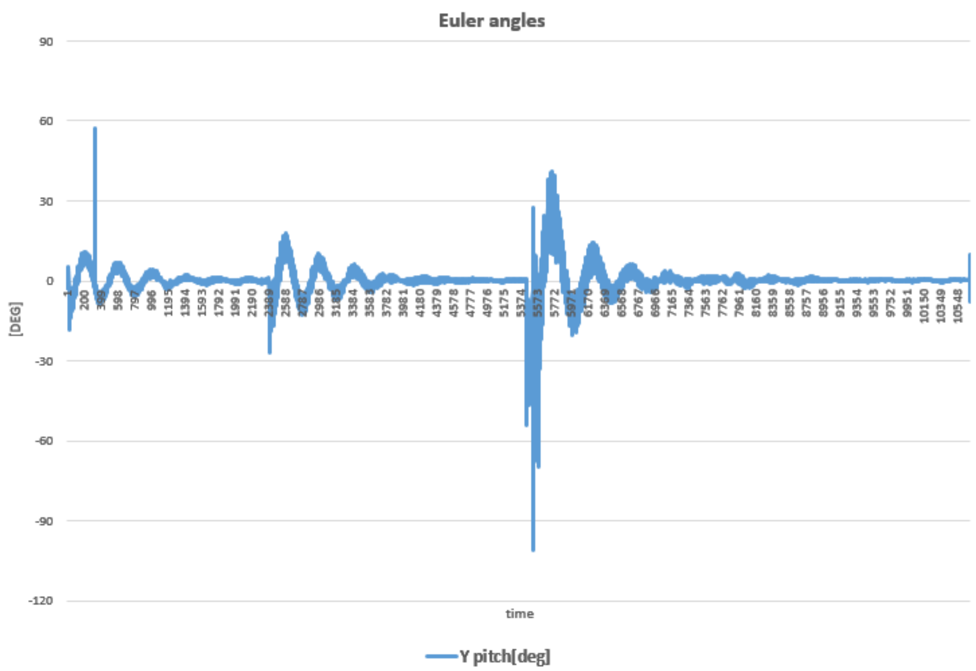

Figure 34: Euler angles representation Y pitch of the time axis from milliseconds

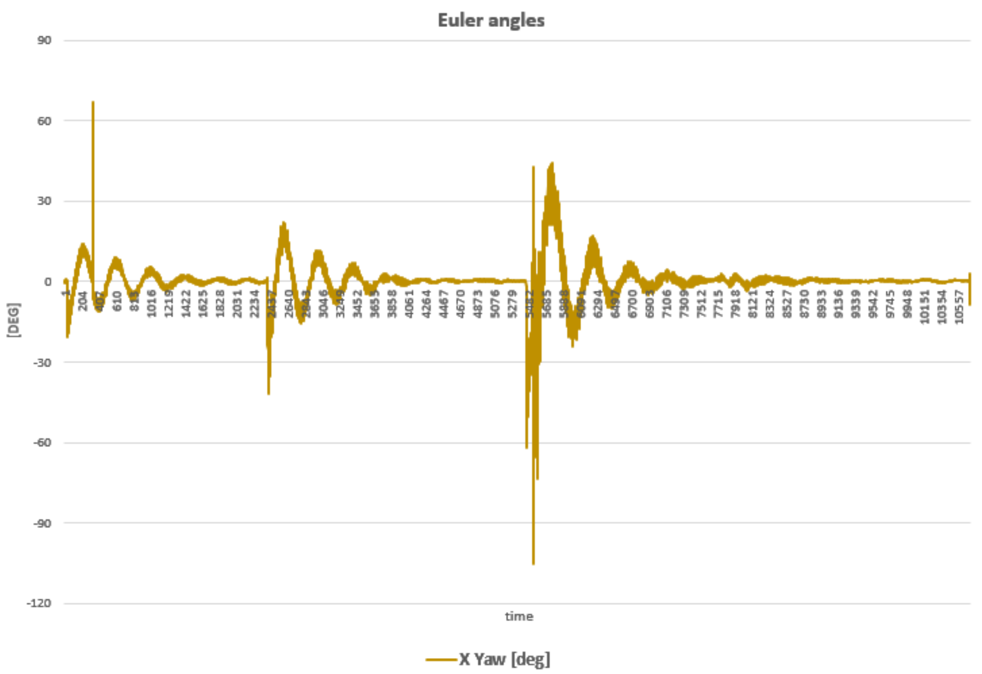

Figure 35: Euler angles representation X yaw of the time axis from milliseconds

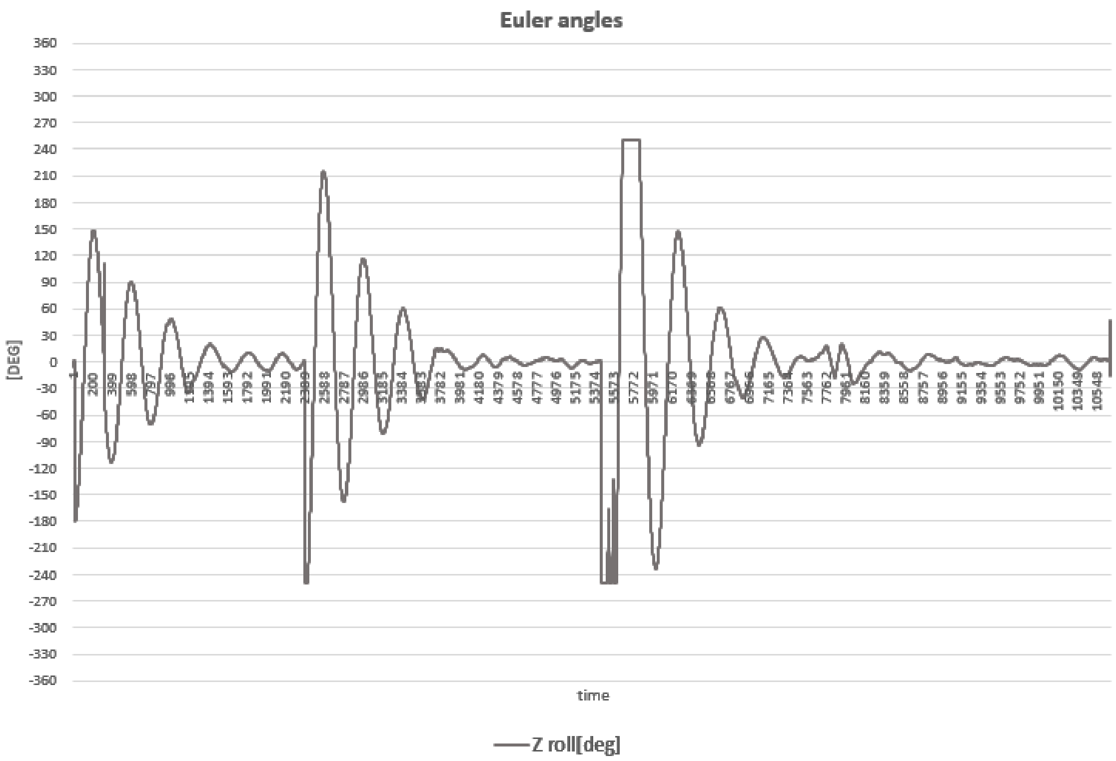

Figure 36: Euler angles representation Z roll of the time axis from milliseconds

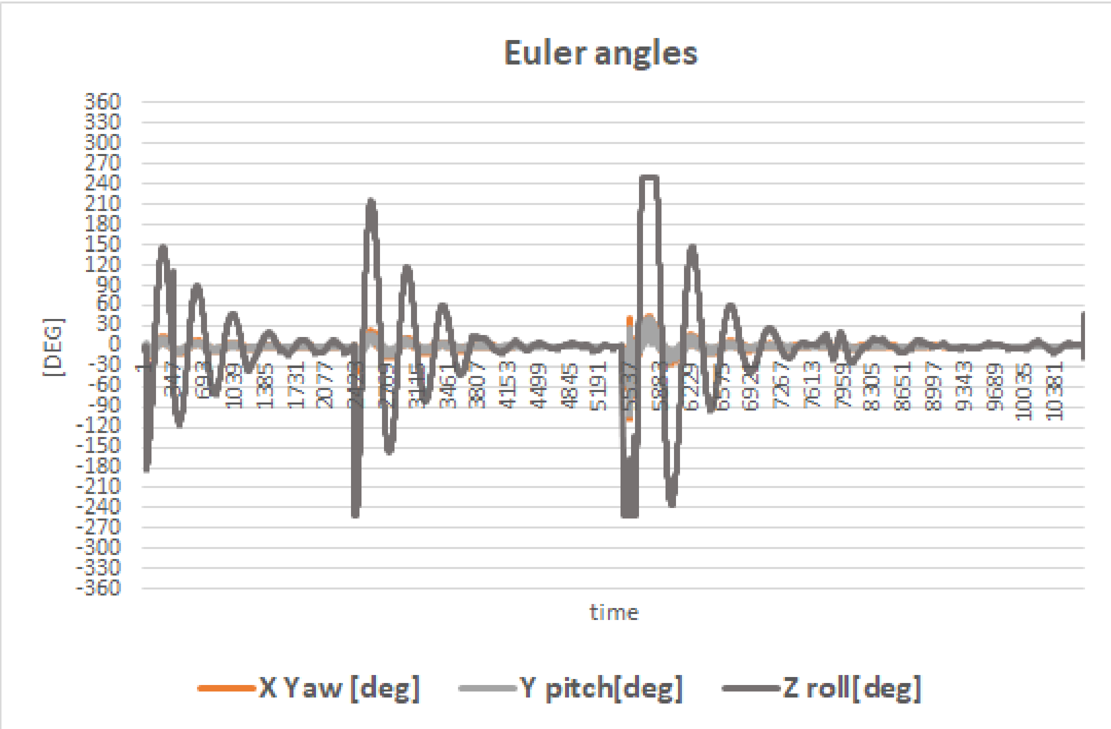

Figure 37: Spin rates in three axis of the time axis from milliseconds

Considering the conditions in the graph, in the first case shown in Figure 38, the external rotation movement is physically applied and continues to move by oscillating. In this case, the system shown in the left column of the rotational angle and rotation angle are shown in the time axis. B-point algorithm damped the rotation of the system applies the PID algorithm at 5 degrees down movement. In this case, more force is applied in large oscillation. In case this test, a disturbing torque applied to the direction of roll axis. The other axis only deteriorated and fluctuations are suppressed in less movement of the roll axis.

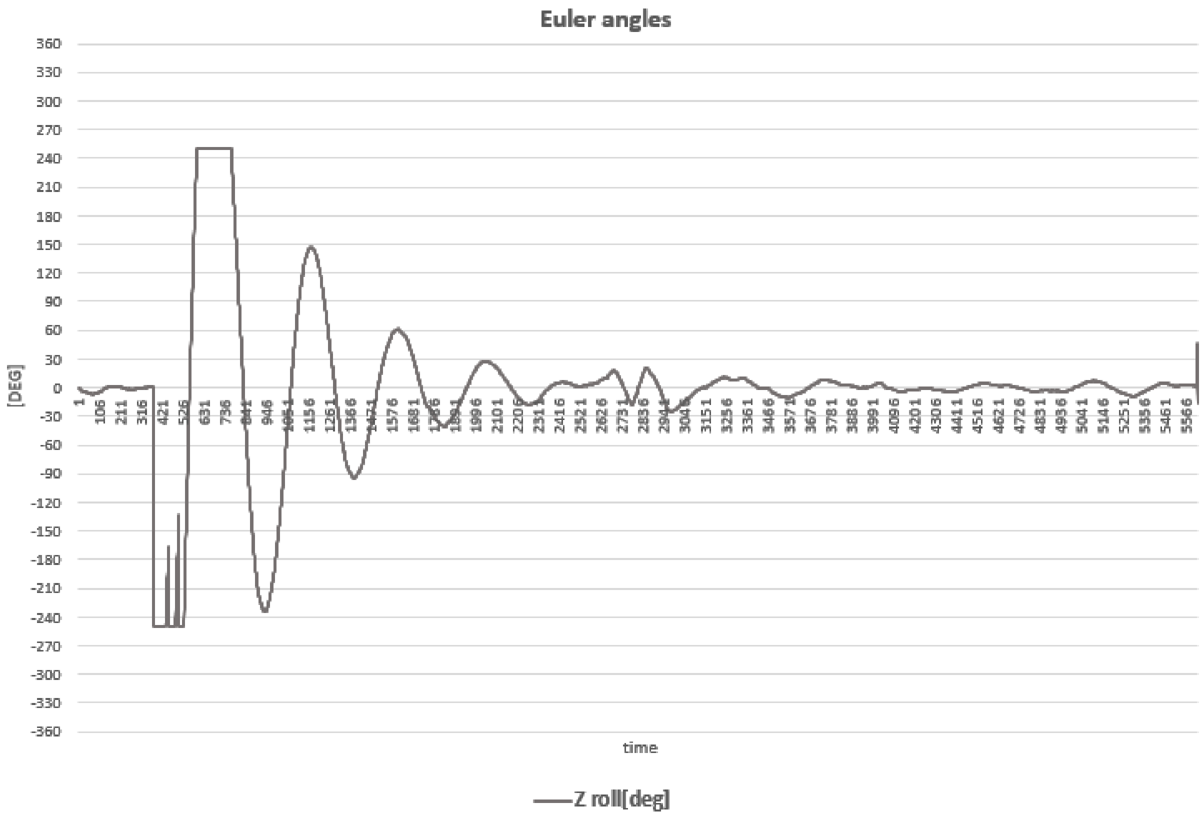

Figure 38: Disturbance torque applied CubeSat body of the time axis from milliseconds

The result of the experiments shows us that such a minimum real-time ADCS system is a good candidate for future near-earth missions and that the three axis CubeSat body can maintain its stable immobility according to yaw, pitch and roll angles. A mildly loaded 3D printed prototype tumbling with 18 rad/sec angular speed could be stabilized in the desired position in just 495 seconds burning average power of 600 mW.

5.2 CubeSat Angels Viewer

An interface software that can work on the computer has been written to better understand the solutions produced while developing the test and system and to observe what is done. 3D visualization of the data coming from the serial port was made using the

Processing language. Yaw, pitch, roll changes are also seen as realtime in the interface software-defined as a ground station in Figure 39. The test setup is seen in realtime at the ground station. When the coils were active, it was seen in Figure 39 that the rotation was damped and stable.

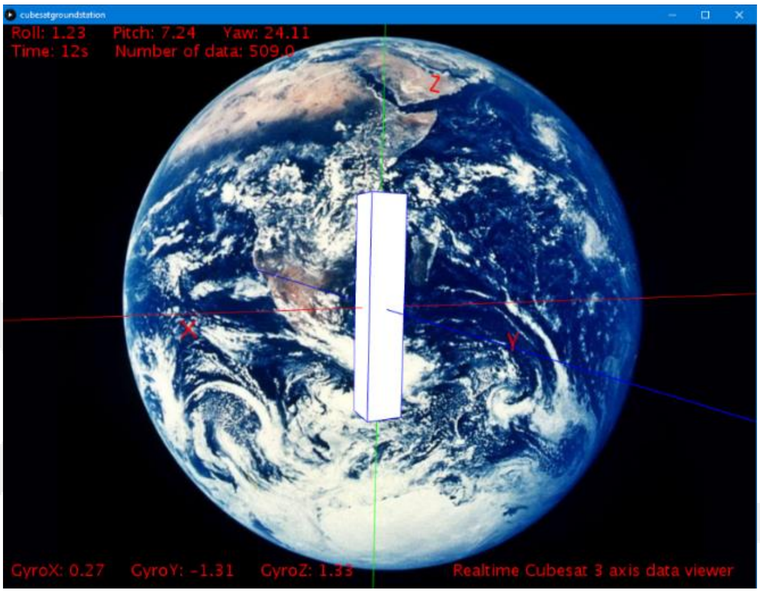

Figure 39: Real-time CubeSat three axis data viewer

CHAPTER VI

CONCLUSIONS

This study presents a prototype of a CubeSat with attitude determination and control system. The proposed solution is especially useful for micro satellites where downsized systems are of great importance.

We have proposed a configurable body frame magnetorquer which had a unique 45-degree offset symmetric body shape to yield an overall more effective control.

In this study, Magnetorquer are consisting of 12 coil areas wrapped in the CubeSat body. The design was experimentally analyzed. The results of the analysis have been confirmed with computer supported observation of the experiments. With the generated magnetic field force, it can be ensured that the CubeSat remains fixed in the desired direction in the orbit or is directed to the desired direction. Coils wrapped on the body frame occupy minimum space, especially for efficient use of the space in CubeSat.

As a result, the design we aimed for the study was carried out with an experimental application and the ideal situation was created with more than one experiment.

FURTHER

As future work, magnetometers can also be incorporated into the same structure with the coils formed by the cross windings. In this case, both the Magnetorquer and the magnetic field can be detected and extra space can be available for aircraft with limited dimensions such as Pico Satellites and CubeSat's.

BIBLIOGRAPHY

[1] X. Xia et al., "NanoSats/CubeSats ADCS survey," 2017 29th Chinese Control And Decision Conference (CCDC), Chongqing, 2017, pp. 5151-5158, doi: 10.1109/CCDC.2017.7979410.

[2] I. Ofodile et al., "ESTCube-2 Attitude Determination and Control: Step Towards Interplanetary CubeSats," 2019 IEEE Aerospace Conference, Big Sky, MT, USA, 2019, pp. 1-12, doi: 10.1109/AERO.2019.8741929.

[3] CubeSats Design Specifications (rev. 12). Pomona, CA: California State Polytechnic University, 2004.

[4] E. Oland, A. Aas, T. M. Steihaug, S. V. Mathisen and F. Vedal, "A design guide for attitude determination and control systems for picosatellites," 2009 4th International Conference on Recent Advances in Space Technologies, Istanbul, 2009, pp. 772-777, doi: 10.1109/RAST.2009.5158295.

[5] A. Ali, M. R. Mughal, H. Ali, L. M. Reyneri and M. N. Aman, "Design, implementation, and thermal modeling of embedded reconfigurable magnetorquer system for nanosatellites," in IEEE Transactions on Aerospace and Electronic Systems, vol. 51, no. 4, pp. 2669-2679, Oct. 2015, doi: 10.1109/TAES.2015.130621.

[6] Francois-Lavet, V. Study of Passive and Active Attitude Control Systems for the OUFTI Nanosatellites. Liege, Belgium: University of Liege Faculty of Applied Sciences, 2009–2010.

[7] 01 05 2020. [Online]. Available: https://www.nanosats.eu/ [Accessed 08 08 2020].

[8] 01 05 2020. [Online]. Available: https://www.nasa.gov/mission_pages/station/research/experiments /explorer/Images/iss051e0448071.jpg [Accessed 08 08 2020].

[9] Kaplan C., "Leo Satellites: Attitude Determination And Control Components ; Some Linear Attitude Control Techniques", M.Sc Thesis, METU 2006

[10] ABBAS, N. N., JUN, L. Y., (t.y.). Design Architecture of Atitude Determination and Control System of ICUBE. 9th Annual Spring CubeSat Developers' Workshop, USA

[11] Liebe, C.C., Murphy, N., Dorsky, L., Udomkesmalee, N., Three-axis sun sensor for attitude determination, IEEE Aerospace and Electronic Systems Magazine, vol. 31, no. 6, pp. 6-11, 2016.

[12] Exact solutions in attitude dynamics of a magnetic dual-spin spacecraft and a generalization of the lagrange top - Scientific Figure on ResearchGate. Available from: https://www.researchgate.net/figure/Single-dipole-model-of-the-Earths-magnetic-field-a-and-the-constant-magnetic-field_fig1_286015031 [accessed 9 Aug, 2020]

[13] 01 05 2020. [Online]. Available: https://www.cubesatshop.com/product/isis-magnetorquer-board/ [Accessed 08 08 2020].

[14] 01 05 2020. [Online]. Available: https://www.space.com/21867-cubesat-deep-space-propulsion-kickstarter.html [Accessed 08 08 2020].

[15] I. Ofodile et al., "ESTCube-2 Attitude Determination and Control: Step Towards Interplanetary CubeSats," 2019 IEEE Aerospace Conference, Big Sky, MT, USA, 2019, pp. 1-12, doi: 10.1109/AERO.2019.8741929.

[16] A. Lassakeur and C. Underwood, "Magnetic Cleanliness Program on CubeSats for Improved Attitude Stability," 2019 9th International Conference on Recent Advances in Space Technologies (RAST), Istanbul, Turkey, 2019, pp. 123-129, doi: 10.1109/RAST.2019.8767816.

[17] B. S. Rani, C. Gomathy, B. Sowmya and R. Narmadha, "Attitude determination and control system of Sathyabamasat," Recent Advances in Space Technology Services and Climate Change 2010 (RSTS & CC-2010), Chennai, 2010, pp. 326-329, doi: 10.1109/RSTSCC.2010.5712821.

[18] Chessab Mahdi, Mohammed & Shehab, Abdal-Razak & Bairmani, Mohammed. (2014). Direct Fuzzy Logic Controller for Nano-Satellite. Journal of Control Engineering and Technology. 4. 210-219. 10.14511/jcet.2014.040307.

[19] A. Ali, M. R. Mughal, H. Ali, L. M. Reyneri and M. N. Aman, "Design, implementation, and thermal modeling of embedded reconfigurable magnetorquer system for nanosatellites," in IEEE Transactions on Aerospace and Electronic Systems, vol. 51, no. 4, pp. 2669-2679, Oct. 2015, doi: 10.1109/TAES.2015.130621.

[20] Z. Mukhtar, A. Ali, M. R. Mughal and L. M. Reyneri, "Design and comparison of different shapes Embedded Magnetorquers for CubeSat Standard Nanosatellites," 2016 International Conference on Computing, Electronic and Electrical Engineering (ICE Cube), Quetta, 2016, pp. 175-180, doi: 10.1109/ICECUBE.2016.7495218.

[21] M. R. Mughal, H. Ali, A. Ali, J. Praks and L. M. Reyneri, "Optimized Design and Thermal Analysis of Printed Magnetorquer for Attitude Control of Reconfigurable Nanosatellites," in IEEE Transactions on Aerospace and Electronic Systems, vol. 56, no. 1, pp. 736-747, Feb. 2020, doi: 10.1109/TAES.2019.2933959.

[22] E. Jerpseth Overby, “Attitude Control for the Norwegian Student Satellite N-Cube”, M.Sc. Thesis in NTNU, 2004

[23] Karataş Soner, “BILSAT-1: Attitude Dynamics and Some Nonlinear Control Techniques”, M.Sc. Thesis in Department of Electrical and Electronics Engineering, METU, 2006.

[24] Hughes, P. C, “Spacecraft Attitude Dynamics”. John Wiley, NY, 1986.

[25] James R. Wertz, "Attitude Prediction" in Spacecraft Attitude Determination and Control, Boston, Kluwer Academic Publishers, 1990, pp. 608-612

[26] E. H. Cayo, R. Duarte and T. Da Silva, "Low cost yaw controller for CubeSat oriented to education and entertainment," 2016 IEEE International Symposium on Consumer Electronics (ISCE), Sao Paulo, 2016, pp. 107-108, doi: 10.1109/ISCE.2016.7797393.

[27] 01 05 2020. [Online]. Available: https://www.pnicorp.com/wp-content/uploads/RM3100-Sensor-Suite-User-Manual-R07-1-2.pdf [Accessed 08 07 2020].

[28] 08 07 2020 [Online]. Available: st.com/resource/en/datasheet/i3g4250d.pdf[Accessed 08 07 2020].

[29] 08 07 2020 [Online]. https://www.analog.com/media/en/technical-documentation/data-sheets/adxl356-357.pdf[Accessed 08 07 2020].

[30] A. H. de Ruiter, C. J. Damaren, and J. R. Forbes. Spacecraft Dynamics and Control An Introduction. John Wiley & Sons, Ltd, 2013.

VITA

Merve Kahyaoğlu was born in 1990 in Izmir. After graduating from high school at Atatürk Anadolu Technical High School, she graduated from Ege University Vocational High School Electronic and Communication Department with second place. She received a B.Sc. degree in Electric and Electronic Engineering from Ege University in 2015. Also, she is a Senior PCB Design Engineer. She has the hard experience of PCB design and manufacture rules so that she has a CID (Certified Interconnect Designer) certified. She has been working at the Vestel Electronic R&D department since 2015.